

# Nonlinear Control of a Continuous Bioreactor Based on Cell Population Model

Mahdi Sharifian, and Mohammad Ali Fanaei

**Abstract**—*Saccharomyces cerevisiae* (baker's yeast) can exhibit sustained oscillations during the operation in a continuous bioreactor that adversely affects its stability and productivity. Because of heterogeneous nature of cell populations, the cell population balance models can be used to capture the dynamic behavior of such cultures. In this paper an unstructured, segregated model is used which is based on population balance equation (PBE) and then in order to simulation, the 4<sup>th</sup> order Rung-Kutta is used for time dimension and three methods, finite difference, orthogonal collocation on finite elements and Galerkin finite element are used for discretization of the cell mass domain. The results indicate that the orthogonal collocation on finite element not only is able to predict the oscillating behavior of the cell culture but also needs much little time for calculations. Therefore this method is preferred in comparison with other methods. In the next step two controllers, a globally linearizing control (GLC) and a conventional proportional-integral (PI) controller are designed for controlling the total cell mass per unit volume, and performances of these controllers are compared through simulation. The results show that although the PI controller has simpler structure, the GLC has better performance.

**Keywords**—Bioreactor, cell population balance, finite difference, orthogonal collocation on finite elements, Galerkin finite element, feedback linearization, PI controller.

## I. INTRODUCTION

**S**ACCHAROMYCES *cerevisiae* (baker's yeast) is one of the important industrial microorganisms which are used in the brewing, food manufacturing and genetic engineering industries. Under moderate operating conditions, continuous bioreactors producing *Saccharomyces cerevisiae* may exhibit sustained oscillations. In most situations, the oscillations adversely affect bioreactor operability. So the underlying cellular mechanisms that cause oscillatory yeast dynamics are still controversial and current topic of study. Understanding and controlling this dynamic behavior would lead to significant advances in yeast production processes. Three types of autonomous oscillations have been reported in literature [1, 2, 3]: cell cycle dependent oscillations, glycolytic oscillations and short-period sustained oscillations. Only the cell cycle dependent oscillations are considered in this paper. These oscillations are also known to be strongly associated with the cell cycle synchronization of the yeast population [3, 4].

Mahdi Sharifian has been graduated in M.S. of chemical engineering from Ferdowsi university of Mashad and he is a process engineer at Regal petrochemical company, Isfahan, Iran (e-mail: mahdi80@gmail.com).

Mohammad Ali Fanaei is with the Chemical Engineering Department, Ferdowsi University of Mashad, Mashad, Iran (corresponding author ; e-mail: fanaei@ferdowsi.um.ac.ir).

Also oscillations are reported to appear at intermediate dissolved oxygen levels [4, 5]. The periods of oscillation varies from 2 to 45 hr depending on the particular strain and operating conditions [4, 6, 7].

Major research efforts have been focused on the characterization of interacellular metabolisms, extracellular media, cell cycle and the interaction of cells with the environment. Depending on these various aspects, a variety of dynamic models have been proposed [3, 8-13]. However no single reported model has been considered satisfactory in addressing all of the complex dynamics that are experimentally observed.

Physically, a yeast culture is comprised of a population of individual cells with different physiological and biochemical properties and an extracellular media with a number of different components. Fredrickson introduced the term "segregated", to indicate explicit accounting for the presence of the heterogeneous individuals in the cell population, and the term "structured" to designate the accounting for the various intracellular and extracellular chemical components. A number of transient models have been proposed to explain the sustained oscillations observed in continuous cultures of baker's yeast. These models can be classified into three categories: structured and unsegregated models; unstructured and segregated models; and structured and segregated models. As unstructured and unsegregated models are over-simplistic and cannot predict the oscillating behavior, they are not considered in the classification. Unsegregated models are based on the simplifying assumption that individual cells have identical physical and chemical properties while segregated models account for differences between individual cells in terms of properties such as cell mass or cell age. Unstructured models have no chemical structure imposed on the biophase i.e. these models are based on the assumption that detailed modeling of intracellular behavior is not essential to describe cell growth. By contrast, structured models account for various chemical components and their interactions within the cell. Therefore structured and unsegregated models consider the biophase as a continuous and well-mixed phase and account for the chemical structure of that [8]. It means that oscillatory dynamics produced by structured, unsegregated models are a direct result of cell metabolism incorporated into the model. For example Jones and Kompala have proposed a structured, unsegregated model to describe the growth dynamics of *S. cerevisiae* in both batch and continuous cultures [9]. The model is derived using the cybernetic modeling framework first proposed by Ramkrishna et al [14]. In cybernetic model, oscillations arise from competition between three pathways: glucose fermentation, glucose oxidation and ethanol oxidation. All three metabolic pathways

have been assumed available for the cell mass growth; however, the metabolic pathway with the highest growth rate dominates the growth. This model is able to produce sustained oscillations over a wide range of operating conditions. Despite this ability, the cybernetic model has a few major drawbacks. First of all, as the model does not account for the segregated nature of cell culture, it can not describe the observed cell cycle synchrony which is believed to play a critical role in the stabilization of the oscillations [1, 5, 15]. Instead, it views the oscillations as a mere result of competitions among metabolic pathways. This explanation is questionable because it is based on the unexplained coincidences that the period of the oscillations matches the characteristic time of the cell cycle and also predicts quick elimination and regeneration of metabolic oscillations in response to the changes in operating conditions such as dilution and agitation rates. Although the dynamic competition between the three metabolic pathways is indeed the causative factor for the oscillations, these predictions are not in accordance with experimental results. In contrast, structured and segregated models [10, 16, 17] attempt to explore the very details of the cell culture. Cells are differentiated individually and oscillations are viewed as a result of cell population dynamics rather than cell metabolism. The model is comprised of a set of cell mass distribution balances combined with a metabolic model that accounts for the basic variables. It is capable of predicting sustained oscillations with periods comparable to those observed experimentally. However, the model solution is quite laborious. Because some model parameters do not have clear physical meaning and can not be determined from experimental measurements. The complexity also makes the model not well suited for practical control applications. Unstructured and segregated models can be viewed as simplifications of the structured and segregated models by ignoring either the intracellular and extracellular chemical structures. Individual cells can be identified by a single variable such as cell age or cell mass. The key feature of these models is a population balance equation (PBE) that explains the time evolution of the cell age or cell mass distribution, combined with mass balance equations of other variables. Although these models cannot capture the interplay between cell metabolism and oscillatory dynamics due to their unstructured nature, they are able to predict the cell cycle synchrony well [18, 19, 20].

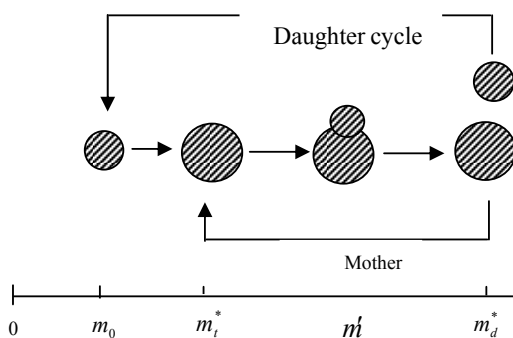


Fig. 1 Simplified cell cycle model for budding yeast

This paper is organized as follows. First, the mathematical model of bioreactor is described. Next, the numerical methods that are used for discretizing the model are described and compared through simulation studies. Finally, two control algorithms, a nonlinear controller based on feedback linearization (globally linearizing control) and a conventional proportional-integral (PI) controller are used for controlling the bioreactor and performances of these controllers are compared through simulation.

## II. MODEL FORMULATION

The model couples the PBE for the cell mass distribution to the substrate mass balance. The simplified cell cycle from which the PBE model is derived is shown in Fig. 1. The PBE is written as [19, 20]:

$$\frac{\partial W(m,t)}{\partial t} + \frac{\partial [K(S')W(m,t)]}{\partial m} = \int_0^\infty 2P(m,m')\Gamma(m',S')W(m',t)dm' - [D + \Gamma(m)]W(m,t) \quad (1)$$

Where:  $m$  is the cell mass;  $W(m,t)$  is the number density of cells with mass  $m$  at time  $t$ ;  $K(S')$  is the single cell growth rate;  $S'$  is the effective substrate concentration;  $P(m,m')$  is the newborn cell probability function;  $\Gamma(m,S')$  is the division intensity function; and  $D$  is the dilution rate.

The division intensity function  $\Gamma(m,S')$  models the tendency of budding cells to divide as they approach a certain critical mass. It has the form [19]:

$$\Gamma(m,S') = \begin{cases} 0 & \text{for } m \leq m_t^* + m_0 \\ \gamma \exp[-\varepsilon(m - m_d^*)^2] & \text{for } m_t^* + m_0 < m < m_d^* \\ \gamma & \text{for } m \geq m_d^* \end{cases} \quad (2)$$

Where  $m_t^*$  is the transition mass,  $m_0$  is the additional mass that mother cells must gain before division is possible,  $\varepsilon$  and  $\gamma$  are constant parameters and  $m_d^*$  is the mass at which the division intensity reaches its maximum value  $\gamma$ . The parameter  $\varepsilon$  determines how rapidly the division rate increases as the cell mass approaches  $m_d^*$ .

The newborn cell probability function  $P(m,m')$  describes the mass distribution of newborn cells resulting from cell division. This function is chosen as [19]:

$$P(m,m') = \begin{cases} A \exp[-\lambda(m - m_t^*)^2] + A \exp[-\lambda(m - m' + m_t^*)^2], & m' > m \text{ and } m' > m_t^* + m_0 \\ 0, & m' \leq m \text{ or } m' \leq m_t^* + m_0 \end{cases} \quad (3)$$

Where  $m$  is the mass of the newborn cell,  $m'$  is the mass of the budding mother cell, and  $A$  and  $\beta$  are constant parameters. This function must satisfy:

$$\int_0^{m'} P(m, m') dm = 1 \quad (4)$$

The probability function produces two identical Gaussian peaks in the cell number distribution, one centered at the transition mass  $m_t^*$  (corresponding to mother cells) and one centered at  $m' - m_t^*$  (corresponding to newborn daughter cells). It has been found that the functions used to model the substrate dependence of the transition mass ( $m_t^*$ ) and the division mass ( $m_d^*$ ) play important roles in the ability of the model to exhibit stable periodic solutions. Therefore, the following functions have been proposed by Zhu et al. [19] for the transition and division masses:

$$m_t^*(S') = \begin{cases} m_{t0} + K_t(S_l - S_h), & S' < S_l \\ m_{t0} + K_t(S' - S_h), & S' \in [S_l, S_h] \\ m_{t0}, & S > S_h \end{cases} \quad (5)$$

$$m_d^*(S') = \begin{cases} m_{d0} + K_d(S_l - S_h), & S' < S_l \\ m_{d0} + K_d(S' - S_h), & S' \in [S_l, S_h] \\ m_{d0}, & S > S_h \end{cases} \quad (6)$$

Where  $S_l, S_h, m_{t0}, m_{d0}, K_t$  and  $K_d$  are constant parameters. The substrate balance is written as [19]:

$$\frac{dS}{dt} = D(S_f - S) - \int_0^\infty \frac{K(S')}{Y} W(m, t) dm \quad (7)$$

Where  $S$  is the actual substrate concentration,  $S'$  is the effective substrate concentration,  $S_f$  is the feed substrate concentration and  $Y$  is a constant yield coefficient. It can be assumed that the single cell growth rate follows the simple Monod kinetics:

$$K(S') = \frac{\mu_m S'}{K_m + S'} \quad (8)$$

Where  $\mu_m$  and  $K_m$  are constant parameters. The filtered (effective) substrate concentration is computed as:

$$\frac{dS'}{dt} = \alpha(S - S') \quad (9)$$

The constant parameter  $\alpha$  determines how fast cells respond to environmental changes.

The parameters values of the bioreactor model (Eqs 1-9) are given in Table I. In addition, the initial cell distribution is assumed to be as below:

$$W(m, 0) = 10^{26} \cdot \exp[-5 \times 10^{26} (m - 6 \times 10^{-13})^2] \quad \text{cells} \cdot \text{g}^{-1} \cdot \text{L}^{-1} \quad (10)$$

TABLE I  
THE PARAMETERS VALUES OF THE CELL POPULATION BALANCE MODEL [19]

Parameter	Value	Parameter	Value
$\gamma$	200	$\varepsilon$	$5 \times 10^{26} \text{ g}^{-2}$
$A$	$\sqrt{25/\pi} \times 10^{13}$	$\lambda$	$100 \times 10^{26} \text{ g}^{-2}$
$S_l$	0.1 g/l	$S_h$	2 g/l
$K_t$	$0.01 \times 10^{-13} \text{ g/g.l}$	$K_d$	$1 \times 10^{-13} \text{ g/g.l}$
$m_{t0}$	$6 \times 10^{-13} \text{ g}$	$m_{d0}$	$11 \times 10^{-13} \text{ g}$
$m_{max}$	$12 \times 10^{-13} \text{ g}$	$m_0$	$1 \times 10^{-13} \text{ g}$
$Y$	0.4	$\mu_m$	$5 \times 10^{-12} \text{ g/h}$
$K_m$	25 g/l	$\alpha$	20
$D$	$0.4 \text{ h}^{-1}$	$S_f$	25 g/l

### III. NUMERICAL SOLUTION

The PBE model is comprised of a coupled set of nonlinear algebraic, ordinary differential and integro-partial differential equations. Analytical solution is possible under very restrictive assumptions [21, 22]. Therefore, numerical solution is required when the PBE model is utilized in open-loop and closed-loop simulations. A variety of numerical solution techniques based on finite difference, weighted residual and orthogonal collocation methods can be applied to such PBE models [23-26]. In this paper three numerical methods: finite difference; orthogonal collocation on finite elements; and Galerkin finite element, are used for solving the bioreactor model equations. In all simulations, a finite cell mass domain,  $0 \leq m \leq m_{max}$ , is chosen in such a way that the number of cells with mass  $m > m_{max}$  is negligible. The implementation algorithms of these numerical methods are mentioned in many textbooks such as Finleysen 1980 [27].

#### A. Finite Difference Method

In this method, the finite mass domain is divided into  $n$  equal space grids. Then the cell population balance equation (Eq. 1) is discretized for each grid and a set of nonlinear ordinary differential equations is obtained for all grids. The backward difference approximation is used for mass dimension derivative due to definite boundary conditions at the first point ( $W(0, t) = 0$ ), and the 1/3 Simpson's rule approximation is used for the integral term [27]. It is important to note that to respect the Simpson's rule, the number of divisions must be even. The concluding set of nonlinear ODEs are:

$$\frac{dW_j}{dt} = -\frac{1}{h} K(S')(W_j - W_{j-1}) \quad (11)$$

$$+ \left(\frac{h}{3}\right) \sum_{i=1}^{n-1} (U_{j,0} + a_i U_{j,i} + U_{j,n}) - (D + \Gamma_j) W_j \quad j=1, 2, \dots, n$$

$$U_{j,i} = 2P_{j,i} \Gamma_i W_i \quad (12)$$

$$\frac{dS}{dt} = D(S_f - S) - \frac{K(S')}{Y} \left( \frac{h}{3} \sum_{i=1}^{n-1} (W_0 + a_i W_i + W_n) \right) \quad (13)$$

$$\frac{dS'}{dt} = \alpha(S - S') \quad (14)$$

$W_j = W(m_j)$  denotes the cell number density at division point  $j$ . The coefficient  $a_i = 2$  for even  $i$  and  $a_i = 4$  for odd  $i$ .  $h$  is the step size of each division.  $P_{j,i} = P(m_j, m_i)$  is the  $(j, i)$  element

of the matrix  $P \in R^{n \times n}$ , and  $\Gamma_i = \Gamma(m_i)$  is the  $i$ th element of the vector  $\Gamma \in R^n$ . Both  $P$  and  $\Gamma$  varying with time as they depend on  $S'$ .

The set of derived ordinary differential equations (Eqs 11, 13 and 14) is solved, using 4<sup>th</sup> order Rung-Kutta with variable step size method (MATLAB 7.0 – ode45).

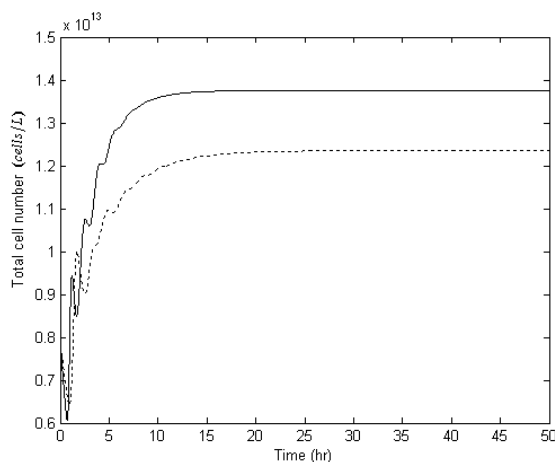


Fig. 2 Open loop transient response of total cell number using finite difference method.  $n=120$ , No oscillatory conditions (line), oscillatory conditions (dash line)

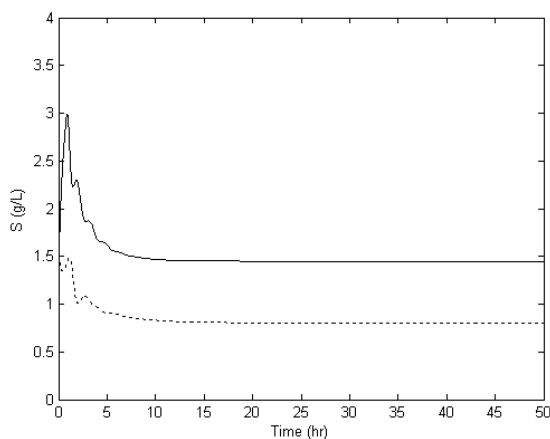


Fig. 3 Open loop transient response of substrate concentration using finite difference method.  $n=120$ , No oscillatory conditions (line), oscillatory conditions (dash line)

The open loop responses of total cell number per unit volume and substrate concentration are shown in Figs. 2 and 3 with 120 number of division and for two cases, oscillatory ( $D = 0.25 \text{ h}^{-1}$ ,  $S_f = 20 \text{ g/l}$ ) and no oscillatory ( $D = 0.4 \text{ h}^{-1}$ ,  $S_f = 25 \text{ g/l}$ ) conditions [19].

As can be seen from the results, the model can not predict the oscillatory behavior if the finite difference method is used. Even by increasing the number of mass domain divisions to 400, oscillation not observed.

#### B. Orthogonal Collocation on Finite Elements

In this method, the finite mass domain is discretized into some elements which may have various step sizes, but due to avoiding complex calculations, these sizes are assumed to be identical. The number of elements is shown by NE. When the solution has steep gradient form it is better to use the different trial functions on each element to approximate solutions. In order to achieve this propose, orthogonal collocation is applied to each element by computing the residuals at each collocation point in the elements [27]. These internal collocation points are determined as the roots of appropriate Jaccobi polynomial and their number is shown by NCOL. Therefore the total number of collocation points on the domain is:

$$NCOL \times NE + NE + 1 = NE(NCOL + 1) + 1 = n \quad (15)$$

After using the above procedure, the following set of ordinary differential equations is developed:

$$\frac{dW_j}{dt} = -\frac{1}{h} K(S') \sum_{i=1}^n A_{j,i} W_i + h \sum_{i=1}^n 2w_i P_{j,i} \Gamma_i W_i - (D + \Gamma_j) W_j, \quad j = 1, 2, \dots, n \quad (16)$$

$$\frac{dS'}{dt} = D(S_f - S) - \frac{K(S')}{Y} h \sum_{i=1}^n w_i W_i \quad (17)$$

$$\frac{dS}{dt} = \alpha(S - S') \quad (18)$$

Where  $A_{n \times n}$  is the collocation matrix [27] and  $h$  is the step size of each element.  $W_j$ ,  $P_{j,i}$  and  $\Gamma_j$  are the same as before.

Integral expressions are approximated using Gaussian quadrature [27]. We use 12 equally spaced finite elements, each with 8 internal collocation points (the total number of collocation points is 109) [19]. The resulting set of ordinary differential equations is solved by ode45. The open loop responses of total cell number per unit volume and substrate concentration are shown in Figs. 4 and 5 for two cases, oscillatory ( $D = 0.25 \text{ h}^{-1}$ ,  $S_f = 20 \text{ g/l}$ ) and no oscillatory ( $D = 0.4 \text{ h}^{-1}$ ,  $S_f = 25 \text{ g/l}$ ) conditions. As can be seen from the results, by using the above numerical method, the model predicts the oscillatory responses. These oscillatory responses have period comparable with reported experimental observations [28].

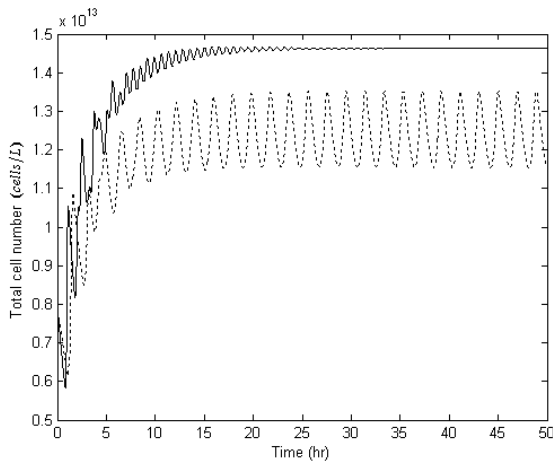


Fig. 4 Open loop transient response of total cell number using Orthogonal collocation on finite elements method.  $n=109$ , No oscillatory conditions (line). oscillatory conditions (dash line)

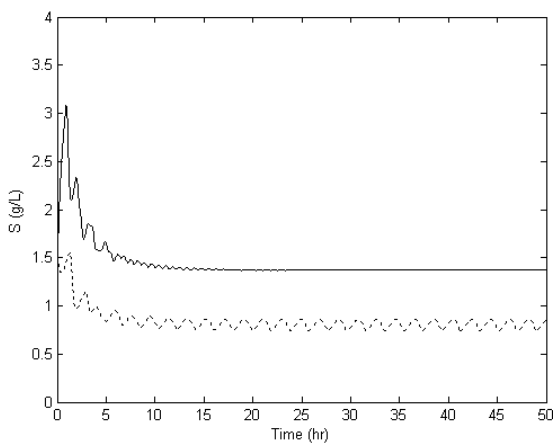


Fig. 5 Open loop transient response of substrate using Orthogonal collocation on finite elements method.  $n=109$ , No oscillatory conditions (line). oscillatory conditions (dash line)

### C. Galerkin Finite Element

This method is similar to orthogonal collocation on finite elements with a difference that the Galerkin method is used on each element of mass domain instead of collocation. Of course, it is possible to apply the same trial function (Jacobi polynomial) but it is common to use the lower order functions (linear or quadratic) [27]. Therefore, linear basic functions are used for discretizing the cell population balance equation. To approximate the integral terms in Eqs (1) and (7), the 1/3 Simpson's rule is applied. After applying the above method, the following set of ordinary differential equations was obtained:

$$\begin{aligned} \frac{dW_i}{dt} = & -\frac{1}{h} K(S^n) \sum_{i=1}^n A_{j,i} W_i \\ & + \left(\frac{h}{3}\right) \sum_{i=1}^{n-1} (U_{j,o} + a_i U_{j,i} + U_{j,n}) - (D + \Gamma_j) W_j, \quad j=1,2,\dots,n \end{aligned} \quad (19)$$

$$U_{j,i} = 2P_{j,i} \Gamma_i W_i \quad (20)$$

$$\frac{dS}{dt} = D(S_f - S) - \frac{K(S^n)}{Y} \left(\frac{h}{3}\right) \sum_{i=1}^{n-1} (W_o + a_i W_i + W_n) \quad (21)$$

$$\frac{dS'}{dt} = \alpha (S - S') \quad (22)$$

Where  $A_{j,i}$  is the Galerkin matrix [27] and  $n$  is the number of elements obtained by discretizing the mass domain.

For solving the above set of differential equations, again ode45 is used. To obtain an accurate solution, the simulation has been performed several times with different number of mass elements. The number of mass elements greater than 200 does not have significant effects on resulting responses. The open loop responses of total cell number per unit volume and substrate concentration are shown in Figs. 6 and 7 with 200 number of elements and for two cases, oscillatory ( $D = 0.25 \text{ h}^{-1}$ ,  $S_f = 20 \text{ g/l}$ ) and no oscillatory ( $D = 0.4 \text{ h}^{-1}$ ,  $S_f = 25 \text{ g/l}$ ) conditions. These solutions show that the model is able to predict the oscillatory dynamics if the Galerkin finite element method is used.

The results of this section show that the finite difference method has drawback in prediction of oscillatory responses and even by increasing the number of mass domain division to 400, no oscillation was observed. Other methods, i.e. orthogonal collocation on finite elements and Galerkin finite element, are able to predict the oscillatory behaviors. The Galerkin finite element method is simpler than the orthogonal collocation but orthogonal collocation is more convergent than Galerkin. For example, Orthogonal collocation on finite elements gets an accurate solution by 109 collocation points on mass domain however Galerkin finite element needs at least 200 division on mass domain to reach this accuracy and it means that the number of calculations is more and the time duration is longer. Therefore the orthogonal collocation on finite element is recommended for solving the PBE models of the yeast culture in continuous bioreactors. Figure 8 shows the cell number distribution as a function of cell mass and time for the oscillatory conditions using orthogonal collocation on finite elements method.

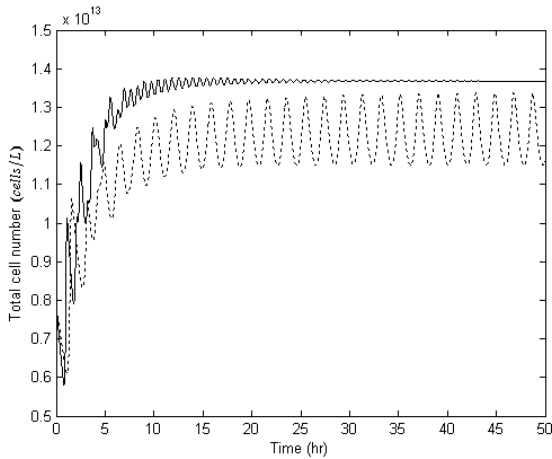


Fig. 6 Open loop transient response of total cell number using Galerkin finite element method.  $n=200$ , No oscillatory conditions (line), oscillatory conditions (dash line)

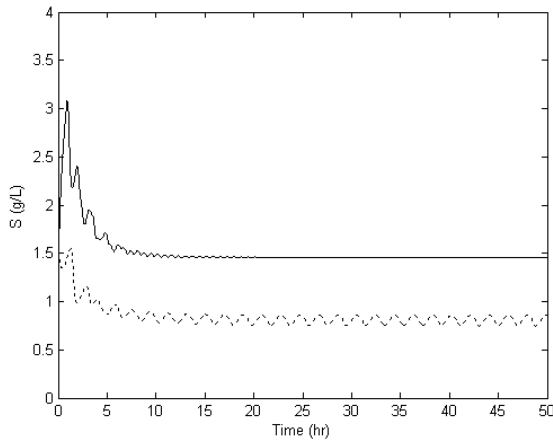


Fig. 7 Open loop transient response of substrate concentration using Galerkin finite element method.  $n=200$ , No oscillatory conditions (line), oscillatory conditions (dash line)

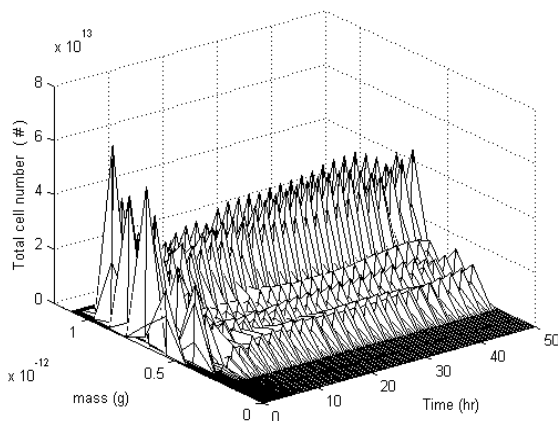


Fig. 8 Cell number distribution using orthogonal collocation on finite elements method

#### IV. CONTROL

Control objectives for oscillating yeast cultures can include the attenuation or the stabilization of the limit cycles. Obviously the attenuation of the undesirable oscillations leads to improve bioreactor operability under normal conditions. Oscillation stabilization may be desirable in certain situations; e.g. to increase the production of key metabolites produced preferentially during a part of the cell cycle. Linear and nonlinear control of oscillating yeast cultures based on model predictive controllers is investigated by many authors [17, 19, 28, 29, 30]. In this paper the oscillation attenuation problem will be investigated based on feedback linearization.

The cell population model contains two variables that may serve as manipulated variables: the dilution rate ( $D$ ) and the feed substrate concentration ( $S_f$ ). The total cell number concentration ( $m_0$ ) and the substrate concentration ( $S$ ) are considered as candidate controlled outputs. Therefore there are a total of four candidate input/output pairings for SISO nonlinear controller design ( $D/m_0$ ,  $D/S$ ,  $S_f/m_0$ ,  $S_f/S$ ). Among them, the  $S_f/m_0$  pair is not used in the controller design. Because that pair has the relative degree of three and the resulted nonlinear controller has complex structure and can not be implemented easily.

In what follows, at first, the globally linearizing control (GLC) algorithm is described briefly. Then, for each pairing, a GLC was designed and the performances of them are compared through simulations. Finally, a conventional PI controller is designed for  $D/m_0$  pair and its performance was compared with GLC. In all simulations a discrete form of controllers with 0.05 hr sampling time was used.

##### A. GLC Method

The GLC method is a nonlinear control algorithm based on differential geometric approach. The first step in the GLC synthesis is the calculation of a state feedback, under which the closed loop input/output system is exactly linear. Then for linearized system, a controller with integral action such as PI can be designed.

To implement the state feedback of the GLC, all the process state variables should be measured or estimated. Open loop or closed loop observers such as extended Kalman filter can be used for estimation of unmeasured state variables [31]. Consider SISO processes with the following model:

$$\begin{cases} \frac{dx}{dt} = f(x) + g(x)u \\ y = h(x) \end{cases} \quad (23)$$

with a finite relative order  $r$  (the relative order is the smallest integer for which  $L_g L_f^{r-1} h(x) \neq 0$ ). Here  $x$  is the vector of state variables,  $u$  and  $y$  are the manipulated input and the controlled output, respectively. Under the state feedback:

$$u = \frac{v - h(x) - \sum_{i=1}^r \beta_i L_f^i h(x)}{\beta_r L_g L_f^{r-1} h(x)} \quad (24)$$

where  $\beta_i$ 's are tunable parameters, the closed loop  $v$ - $y$  behavior is linear and described by the following equation:

$$v = y + \sum_{i=1}^r \beta_i \frac{d^i y}{dt^i} \quad (25)$$

Some guidelines for tuning of  $\beta_i$ 's parameters and other remarks for using GLC method are described by Soroush and Kravaris [32].

#### B. Control based on D/S Pair

For the D/S pair, the control law of the GLC is synthesized directly from the substrate equation (which has the relative order one):

$$\frac{dS}{dt} = D(S_f - S) - \frac{K(S')}{Y} \int_0^\infty W(m,t) dm \quad (26)$$

Therefore, the control law has the following form:

$$D = \frac{v - S + \beta \frac{K(S')}{Y} \int_0^\infty W(m,t) dm}{\beta(S_f - S)} \quad (27)$$

It is necessary to know that the integral term in the above equations (26, 27) represents the total number of cells per unit volume ( $m_0 = \int_0^\infty W(m,t) dm$ ). A PI controller can be used to generate the input of linearized system ( $v$ ) as given below:

$$v(t) = v_s + K_c(S^* - S) + \frac{K_c}{\tau_I} \int_0^t (S^* - S) dt \quad (28)$$

Where  $S^*$  is the desired profile of substrate concentration in the bioreactor.  $K_c$  and  $\tau_I$  are gain and integral time constant of PI controller, respectively.

The resulting control algorithm (GLC), have three parameters  $\beta$ ,  $K_c$  and  $\tau_I$  that must be tuned. These parameters are tuned with trial and error. The resulted values are:  $K_c=1$ ,  $\beta=1hr$  and  $\beta=1hr$ . In implementation of the above algorithm, the substrate concentration can be measured on-line, but the total cell number per unit volume can not be measured on-line. Therefore, in all simulation, an open loop observer is used for estimation of  $m_0$ . The responses of  $m_0$  and  $S$  are shown in Figs. 9 and 10 for two cases: a) the D/S pair loop is open ( $S_f=20$  g/l,  $D=0.25$  hr<sup>-1</sup>), and b) after 5 hours, the D/S pair loop is closed ( $S_f=20$  g/l,  $S^*=0.8$  g/l). As can be seen from the results, although the oscillation in the substrate concentration is damped, the oscillation in the total cell number is not damped, and therefore the D/S pair control is not suitable for the attenuation of oscillation.

#### C. Control based on S<sub>f</sub>/S Pair

In this case, the control law of GLC method which is synthesized directly from the substrate equation has the following form:

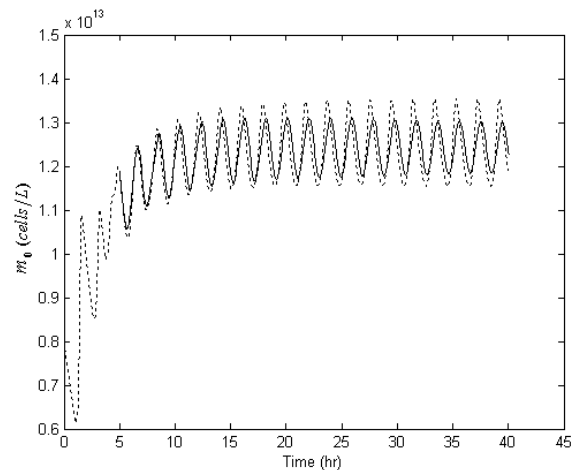


Fig. 9 Transient response of total cell number per unit volume. D/S pair loop is open (dash line), D/S pair loop is closed using a GLC (line)

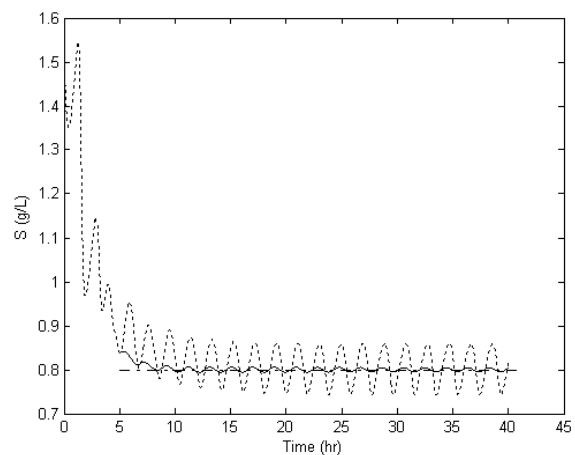


Fig. 10 Transient response of substrate concentration. D/S pair loop is open (dash line), D/S pair loop is closed using a GLC (line)

$$S_f = \frac{v - S + \beta \frac{K(S')}{Y} \int_0^\infty W(m,t) dm}{\beta D} + S \quad (29)$$

In the same as before, the input of linearized model ( $v$ ) can be generated by a PI controller (Eq 28). In addition, the same values as before are assumed for the GLC parameters ( $K_c=1$ ,  $\tau_I=1hr$  and  $\beta=1hr$ ). The responses of  $m_0$  and  $S$  are shown in Figs. 11 and 12 for two cases: a) the S<sub>f</sub>/S pair loop is open ( $S_f=20$  g/l,  $D=0.25$  hr<sup>-1</sup>), and b) after 5 hours, the S<sub>f</sub>/S pair loop is closed ( $D=0.25$  hr<sup>-1</sup>,  $S^*=0.8$  g/l). As can be seen from the results, although the oscillation in the substrate concentration is damped, the oscillation in the total cell number is not damped, and therefore in the same as D/S pair, the S<sub>f</sub>/S pair control is not suitable for the attenuation of oscillation.

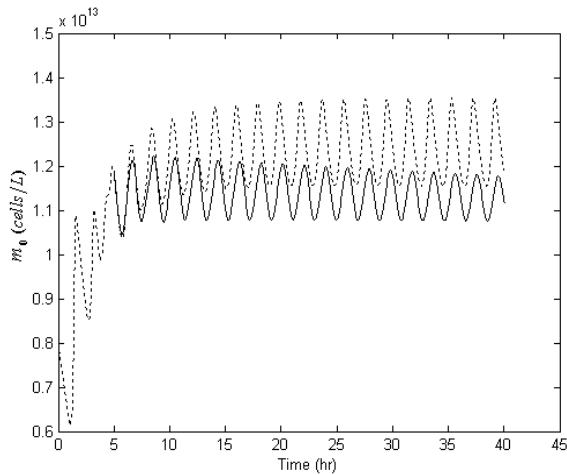


Fig. 11 Transient response of total cell number per unit volume.  $S_f/S$  pair loop is open (dash line),  $S_f/S$  pair loop is closed using a GLC (line)

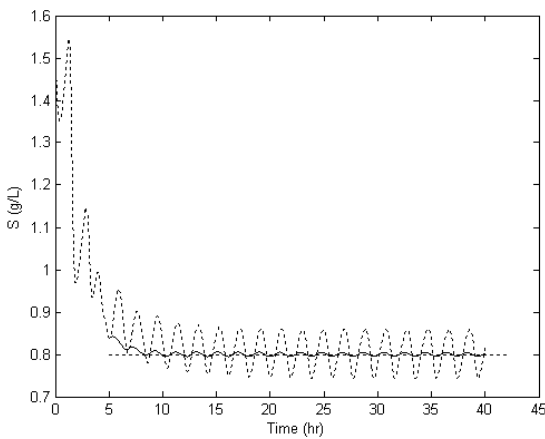


Fig. 12 Transient response of substrate concentration.  $S_f/S$  pair loop is open (dash line),  $S_f/S$  pair loop is closed using a GLC (line)

#### D. Control based on $D/m_0$ Pair

By integrating the equation (1) with respect to  $m$ , the differential equation describing the evolution of the total cell number per unit volume is easily derived as below:

$$\frac{dm_0}{dt} = \int_0^\infty \int_0^\infty 2P(m, m') \Gamma(m', S') W(m', t) dm' dm - \int_0^\infty \Gamma(m, S') W(m, t) dm - Dm_0 \quad (30)$$

Therefore, the control law of the GLC has the following form:

$$D = \frac{-1}{\beta m_0} \{ v - m_0 - \beta [\int_0^\infty \int_0^\infty 2P(m, m') \Gamma(m', S') W(m', t) dm' dm - \int_0^\infty \Gamma(m, S') W(m, t) dm] \} \quad (31)$$

The input of the linearized system ( $v$ ) can be generated by a PI controller as below:

$$v(t) = v_s + K_c(m_0^* - m_0) + \frac{K_c}{\tau_I} \int_0^t (m_0^* - m_0) dt \quad (32)$$

Where  $m_0^*$  is the desired profile of the total cell number per unit volume. The same values as before are assumed for the GLC parameters ( $K_c=1$ ,  $\tau_I=1hr$  and  $\beta=1hr$ ).

The responses of  $m_0$  and  $S$  are shown in Figs. 13 and 14 for two cases: a) the  $D/m_0$  pair loop is open ( $S_f=20$  g/l,  $D=0.25$  hr<sup>-1</sup>), and b) after 5 hours, the  $D/m_0$  pair loop is closed ( $S_f=20$  g/l,  $m_0^* = 1.3 \times 10^{13}$  cells/l). As can be seen from the results, the GLC controller based on  $D/m_0$  pair not only is able to control the total cell number per unit volume but also damp the oscillation in the substrate concentration. Therefore the  $D/m_0$  pair control is suitable for the attenuation of oscillation. To distinguish the abilities and disabilities of the proposed nonlinear controller (GLC), a conventional PI controller is used for  $D/m_0$  pair. The parameters of this PI controller are tuned with trail and error and have the following values:  $K_c = -1.5$  hr<sup>-1</sup>,  $\tau_I = 1hr$ . It is necessary to note that, a scaled value of error is used for input of the PI controller (error =  $[m_0^* - m_0] / m_0^*$ ). The closed loop response of  $m_0$  and  $D$  are shown in Figs. 15 and 16 for GLC and PI controller. In these figures, the controller is turn on after 5 hours and a step change in setpoint is applied after 35 hours (desired value of  $m_0$  is changed from  $1.3 \times 10^{13}$  to  $1 \times 10^{13}$  cells/l). As can be seen from the results, the proposed GLC method has much better performances than conventional PI controller.

It is necessary to note that, the total cell number per unit volume is unobservable from substrate concentration measurements. Therefore, as mentioned before, an open loop observer is used in implementation of GLC method. With respect to this fact, the performance of GLC method will decrease with increasing the model mismatch.

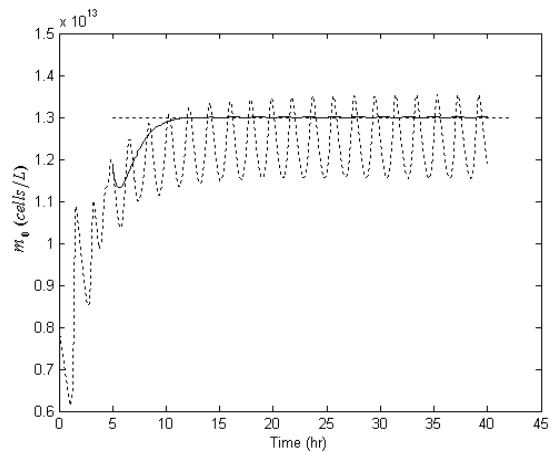


Fig. 13 Transient response of total cell number per unit volume.  $D/m_0$  pair loop is open (dash line),  $D/m_0$  pair loop is closed using a GLC (line)



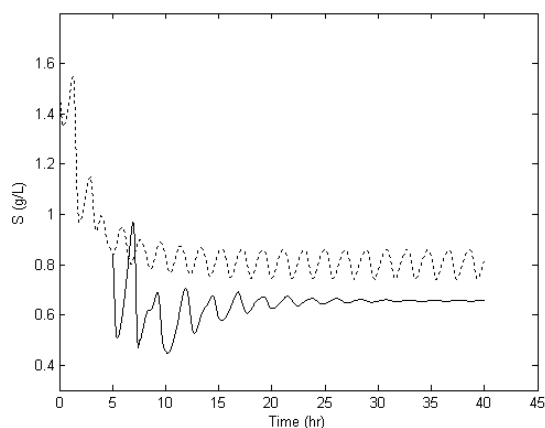


Fig. 14 Transient response of substrate concentration.  $D/m_0$  pair loop is open (dash line),  $D/m_0$  pair loop is closed using a GLC (line)

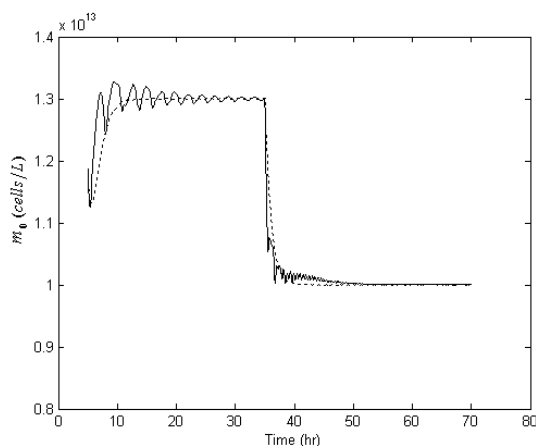


Fig. 15 Closed loop response of total cell number per unit volume, GLC method (dash line), PI controller (line)

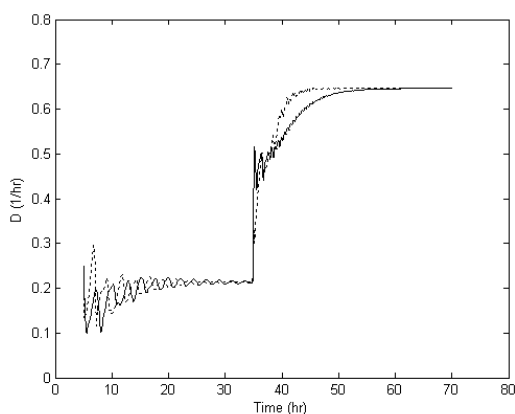


Fig. 16 Closed loop response of dilution rate, GLC method (dash line), PI method (line)

## V. CONCLUSION

In this paper, the numerical solution of a cell population balance model which proposed for a continuous bioreactor, and nonlinear control of the simulated model have been investigated. This investigation is performed when the stable oscillation exist in the continuous yeast culture.

The numerical solution has two steps. In the first step, the cell population balance equation is discretized over the finite cell mass domain by using three numerical methods of finite difference, orthogonal collocation on finite elements and Galerkin finite element. Then the resulted set of ordinary differential equations is solved numerically by 4<sup>th</sup> order Runge Kutta (ode45 of MATLAB 7.0) over the time domain. The results show that the finite difference method has drawback in prediction of oscillatory responses and even by increasing the number of mass domain division to 400, no oscillation was observed. Orthogonal collocation on finite elements and Galerkin finite element are able to predict the oscillatory behaviors. The Galerkin finite element method is simpler than the orthogonal collocation but orthogonal collocation is more convergent than Galerkin. For example, Orthogonal collocation on finite elements gets an accurate solution by 109 collocation points on mass domain however Galerkin finite element needs at least 200 division on mass domain to reach this accuracy and it means that the number of calculations is more and the time duration is longer. Therefore the orthogonal collocation on finite element is recommended for solving the PBE models of the yeast culture in continuous bioreactors.

Three nonlinear controllers with GLC structure are designed for controlling the  $D/S$ ,  $S/S$  and  $D/m_0$  pairs. The results show that the oscillation behavior of the total cell number per unit volume can not be damped by controlling the  $D/S$  or  $S/S$  pairs. But the GLC controller based on  $D/m_0$  pair not only is able to control the total cell number per unit volume but also damp the oscillation in the substrate concentration. Therefore the  $D/m_0$  pair control is recommended for the attenuation of oscillation. Finally the performance of GLC is compared with a conventional PI for controlling the  $D/m_0$  pair. The results show that although the PI controller has simpler structure, the GLC controller has better performance. It is necessary to note that, the total cell number per unit volume is unobservable from substrate concentration measurements. Therefore, an open loop observer is used in implementation of GLC method. With respect to this fact, the performance of GLC method will decrease with increasing the model mismatch.

## REFERENCES

- [1] T. Munch, B. Sonnleitner, and A. Fiechter, "New insights into the synchronization mechanism with forced synchronous cultures of *Saccharomyces cerevisiae*", *J. Biotechnol.*, 24, p299-313, 1992.
- [2] S. J. Parulekar, G. B. Semones, M. J. Rolf, J. C. Lievens, and H. C. Lim, "Induction and elimination of oscillations in continuous cultures of *Saccharomyces cerevisiae*", *Biotechn. Bioeng.*, 28, p700-710, 1986.
- [3] P. R. Patnaik, "Oscillatory metabolism of *Saccharomyces cerevisiae*: an overview of mechanisms and models", *Biotechnology Advances*, 21, p183-192, 2003.
- [4] C. Strassle, B. Sonnleitner, and A. Fiechter, "A predictive model for the spontaneous synchronization of *Saccharomyces cerevisiae* grow in

- continuous culture. II. Experimental verification", *J. Biotechnol.*, 9, p191-208, 1989.
- [5] D. E. Porro, B. Martegani, M. Ranzi, and L. Alberghina, "Oscillations in continuous cultures of budding yeasts: A segregated parameter analysis", *Biotechnol. Bioeng.*, 32, p411-417, 1988.
- [6] T. Munch, B. Sonnleitner, and A. Fiechter, "The decisive role of the *Saccharomyces cerevisiae* cell cycle behavior for dynamic growth characterization", *J. Biotechnol.*, 22, p329-352, 1992.
- [7] M. Beuse, R. Bartling, A. Kopmann, H. Diekmann, and M. Thoma, "Effect of the dilution rate on the mode of oscillation in continuous cultures of *Saccharomyces cerevisiae*", *J. of Biotechnology*, 61, p15-31, 1998.
- [8] L. Cazzador, L. Mariani, E. Martegani, and L. Alberghina, "Structured segregated models and analysis of self-oscillating yeast continuous cultures", *Bioprocess Eng.*, 5, p175-180, 1990.
- [9] K. D. Jones, and D. S. Kompala, "Cybernetic model of the growth dynamics of *Saccharomyces cerevisiae* in batch and continuous cultures", *J. Biotechnology*, 71, p105-131, 1999.
- [10] E. Martegani, D. Porro, B. M. Ranzi, and L. Alberghina, "Involvement of a cell size control mechanism in the induction and maintenance of oscillations in continuous cultures of budding yeast", *Biotechnol. Bioeng.*, 36, p453-459, 1990.
- [11] C. Strassle, B. Sonnleitner, and A. Fiechter, "A predictive model for the spontaneous synchronization of *Saccharomyces cerevisiae* grown in continuous culture. I. Concept", *J. Biotechnol.*, 7, p299-318, 1988.
- [12] N. V. Mantzaris, F. Sreenc, and P. Daoutidis, "Nonlinear productivity control using a multi-stage cell population balance model", *Chem. Eng. Sci.*, 57, p1-14, 2002.
- [13] A. G. Fredrickson, and N. V. Mantzaris, "A new set of population balance equations for microbial and cell cultures", *Chem. Eng. Sci.*, 57, p2265-2278, 2002.
- [14] D. Ramkrishna, D. S. Kompala, and G. T. Tsao, "Are microbes optimal strategists?", *Biotechnol. Prog.*, 3, p121-126, 1987.
- [15] J. D. Sheppard, and P. S. Dawson, "Cell synchrony and periodic behavior in yeast populations", *Canadian J. Chem. Eng.*, 77, p893-902, 1999.
- [16] Y. Zhang, M. A. Henson, and Y.G. Kevrekidis, "Nonlinear model reduction for dynamic analysis of cell population models", *Chem. Eng. Sci.*, 58, p429-445, 2003.
- [17] M. A. Henson, "Dynamic modeling and control of yeast cell populations in continuous biochemical reactors", *Comp. Chem. Eng.*, 27, p1185-1199, 2003.
- [18] N. V. Mantzaris, P. Daoutidis, "Cell population balance modeling and control in continuous bioreactors", *J. Process Control*, 14, p775-784, 2004.
- [19] G. Y. Zhu, A. M. Zamamiri, M. A. Henson, and M. A. Hjortso, "Model predictive control of continuous yeast bioreactors using cell population models", *Chem. Eng. Sci.*, 55, p6155-6167, 2000.
- [20] Y. Zhang, *Dynamic modeling and analysis of oscillatory bioreactors*, PhD Theses, Louisiana State University, Chem. Eng. Department, 2002.
- [21] M. A. Hjortso, and J. Nielsen, "A conceptual model of autonomous oscillations in microbial cultures", *Chem. Eng. Sci.*, 49, p1083-1095, 1994.
- [22] M. A. Hjortso, and J. Nielsen, "Population balance models of autonomous microbial oscillations", *J. Biotechnol.*, 42, p255-269, 1995.
- [23] N. V. Mantzaris, J. J. Liou, P. Daoutidis, and F. Sreenc, "Numerical solution of a mass structured cell population balance model in an environment of changing substrate concentration", *J. Biotechnol.*, 71, p157-174, 1999.
- [24] N. V. Mantzaris, P. Daoutidis, and F. Sreenc, "Numerical solution of multi-variable cell population balance models: I. Finite difference methods", *Comp. Chem. Eng.*, 25, p1411-1440, 2001.
- [25] N. V. Mantzaris, P. Daoutidis, and F. Sreenc, "Numerical solution of multi-variable cell population balance models: II. Spectral methods", *Comp. Chem. Eng.*, 25, p1441-1462, 2001.
- [26] N. V. Mantzaris, P. Daoutidis, and F. Sreenc, "Numerical solution of multi-variable cell population balance models: III. Finite element methods", *Comp. Chem. Eng.*, 25, p1463-1481, 2001.
- [27] B. A. Finlayson, *Nonlinear analysis in chemical engineering*, McGraw-Hill, 1980.
- [28] M. J. Kurtz, G. Y. Zhu, A. M. Zamamiri, M. A. Henson, and M. A. Hjortso, "Control of oscillating microbial cultures described by population balance models", *Ind. Eng. Chem. Research*, 37, p4059-4070, 1998.
- [29] Y. Zhang, A. M. Zamamiri, M. A. Henson, and M. A. Hjortso, "Cell population models for bifurcation analysis and nonlinear control of continuous yeast bioreactors", *J. process control*, 12, p721-734, 2002.
- [30] M. J. Kurtz, G. Y. Zhu, A. M. Zamamiri, M. A. Henson, and M. A. Hjortso, "Control of oscillating microbial cultures described by population balance models", *Ind. Eng. Chem. Research*, 37, p4059-4070, 1998.
- [31] M. Shahrokhi, and M. A. Fanaei, "State estimation in a batch suspension polymerization reactor", *Iranian Polymer J.*, 10, p173-187, 2001.
- [32] M. Soroush, and C. Kravaris, "Nonlinear control of a batch polymerization reactor: An experimental study", *AIChE J.*, 38, p1429-1440, 1992.